

Improving compatibility between thermoelectric components through current refraction

K Song(宋坤), H P Song(宋豪鹏), C F Gao(高存法)

Citation: Chin. Phys. B . 2018, 27(7): 077304. **doi:** 10.1088/1674-1056/27/7/077304

Journal homepage: http://cpb.iphy.ac.cn; http://iopscience.iop.org/cpb

What follows is a list of articles you may be interested in

Macro-performance of multilayered thermoelectric medium

Kun Song(宋坤), Hao-Peng Song(宋豪鹏), Cun-Fa Gao(高存法)

Chin. Phys. B . 2017, 26(12): 127307. **doi:** 10.1088/1674-1056/26/12/127307

Generating and reversing spin accumulation by temperature gradient in a quantum dot attached to ferromagnetic leads

Bai Xu-Fang, Chi Feng, Zheng Jun, Li Yi-Nan

Chin. Phys. B . 2012, 21(7): 077301. **doi:** 10.1088/1674-1056/21/7/077301

Signature of symmetry of laterally coupled quantum dots in far-infrared spectrum

Gu Li-Ying,Li Yan-Fang,Chu Wei-Dong,Wei Ying-Hui

Chin. Phys. B . 2012, 21(2): 027301. **doi:** 10.1088/1674-1056/21/2/027301

Quasibound states in graphene quantum-dot nanostructures generated by concentric potential barrier rings

Jiang Zhao-Tan,Yu Cheng-Long,Dong Quan-Li

Chin. Phys. B . 2012, 21(2): 027303. **doi:** 10.1088/1674-1056/21/2/027303

Quantum computation with two-dimensional graphene quantum dots

Li Jie-Sen, Li Zhi-Bing, Yao Dao-Xin

Chin. Phys. B . 2012, 21(1): 017302. **doi:** 10.1088/1674-1056/21/1/017302

Improving compatibility between thermoelectric components through current refraction*

K Song(宋坤), H P Song(宋豪鹏)†, and C F Gao(高存法)

State Key Laboratory of Mechanics and Control of Mechanical Structures, Nanjing University of Aeronautics & Astronautics, Nanjing 210016, *China*

(Received 10 January 2018; revised manuscript received 11 April 2018; published online 25 June 2018)

It is well known that components with dissimilar compatibility factors cannot be combined by segmentation into an efficient thermoelectric generator, since each component needs a unique optimal current density. Based on the complex variable method, the thermal-electric field within a bi-layered thermoelectric composite has been analyzed, and the field distributions have been obtained in closed-form. Our analysis shows that current refraction occurs at the interface, both the refraction angle and current density vary with the incidence angle. Further analysis proves that the current densities in two components can be adjusted independently by adjusting the incidence current density and incidence angle, thus the optimal current density can be matched in both components, and the conversion efficiency can be significantly increased. These results point to a new route for high efficiency thermoelectric composites.

Keywords: thermoelectric material, current refraction, compatibility factor, conversion efficiency

PACS: 73.50.Lw, 84.60.Rb, 84.60.Bk, 46.25.Cc **DOI:** 10.1088/1674-1056/27/7/077304

1. Introduction

Thermoelectric materials have great advantages due to their specific ability of converting heat directly into electricity, and vice versa, and thus they are widely used in many fields, such as modern industry,[1–4] military,[5,6] and protection of the environment.[7–9] The performance of a thermoelectric material is represented by figure of merit ZT, which is deduced from electric conductivity σ, thermal conductivity κ, and Seebeck coefficient S as[10]

$$ZT = \frac{\sigma S^2}{\kappa} T. \tag{1}$$

A great deal of effort has been devoted to adjusting the material properties, since a high figure of merit needs high electric conductivity and Seebeck coefficient while low thermal conductivity. For example, the thermoelectric performance of $AgPb_mSbTe_{m+2}$ was maximized by optimizing the spark plasma sintering temperature.[11] Zhang *et al.*[12] enhanced the thermoelectric performance of Se-doped PbTe bulk materials via nanostructuring and multi-scale hierarchical architecture. The thermoelectric property of $Cu_{1.8}S$ was improved via introducing Bi_2S_3 and Bi_2S_3Bi core-shell nanorods.[13] The high ZT Si nanowires were processed by a wafer-scale manufacturing technique.[14] Chen *et al.*[15,16] significantly reduced the thermal conductivity of silicon nanowires (SiNWs) and germanium nanowires. Besides, many researchers focused on developing hybrid thermoelectric composites, since it is rather difficult to satisfy competing requirements on thermoelectric properties for high conversion efficiency in a single-phase material. Mahan and Lyod[17] designed a layered thermoelectric device using semiconductor quantum wells. The thermoelectric properties of alternatively layered films of polyaniline were studied by Yan and Toshima.[18] A bulk thermoelectric cooler was designed by Antonik *et al.* by employing thin-film thermoelectric materials sandwiched between plastic substrates.[19] The routes for enhanced performance of thermoelectric materials by incorporating nanostructures within the bulk materials was discussed by Rao *et al.*[20]

Quite a few continuum models have been developed to understand the overall efficiency of thermoelectric composites. Snyder and Ursell[21] deeply discussed the thermoelectric efficiency and compatibility, and proved that components with dissimilar compatibility factors cannot be combined by segmentation into an efficient thermoelectric generator. Song textitet al.[22] analyzed the unavoidable electric current caused by inhomogeneities and its influence on measured material parameters of thermoelectric materials. Rigorous continuum analysis has also been carried out for one-dimensional parallel[23] and layered[24–26] thermoelectrics, wherein the conception of optimal electric current is proposed, and thus the conversion efficiency of a composite can be slightly higher than its constituents as the optimal current density can be matched everywhere by tailoring the material properties. These analyses, however, were based on the model that the electric current always flows through the interface vertically and retains its direction. As such, components with dissimilar compatibility factors (or optimal current density) cannot be combined into an efficient thermoelectric generator, which greatly restricts the component matching of composite thermoelectric materials. It is thus highly desirable if arbitrary

*Project supported by the Fundamental Research Funds for the Central Universities, China (Grant No. NS2016008).

†Corresponding author. E-mail: hpsong@nuaa.edu.cn

© 2018 Chinese Physical Society and IOP Publishing Ltd

components can fit together and work well.

In this work, the problem of current refraction at the interface is studied. We attempt to derive a method that can greatly improve the compatibility of the components. Our results show that the current density in each component can be adjusted independently by adjusting the incidence current density and incidence angle, therefore components with dissimilar compatibility factors can also be combined into efficient thermoelectric generators. These results point to a new route for high efficiency thermoelectric composites.

2. Two-dimensional thermoelectric problems

2.1. Governing equations of thermoelectric material

We consider the coupled transports of heat and electricity in a thermoelectric medium, within which the electric current density $\boldsymbol{J}$ is coupled with the heat flux $\boldsymbol{J}_Q$ through the Seebeck coefficient S[27,28]

$$-\boldsymbol{J}=\sigma\nabla\phi+\sigma S\nabla T, \tag{2}$$

$$\boldsymbol{J}_Q=TS\boldsymbol{J}-\kappa\nabla T, \tag{3}$$

where T and ϕ are the temperature and the electric potential, respectively. The total energy is transported by both electrons and heat in thermoelectric materials, and can be derived as

$$\boldsymbol{J}_E=\boldsymbol{J}_Q+\phi\boldsymbol{J}=(\phi+ST)\,\boldsymbol{J}-\kappa\nabla T. \tag{4}$$

We limit ourselves to systems wherein both charges and energy are conserved, such that both current density and energy flux are divergence-free,

$$\nabla\cdot\boldsymbol{J}=0, \tag{5}$$

$$\nabla\left(\boldsymbol{J}_Q+\phi\boldsymbol{J}\right)=0. \tag{6}$$

It is worth pointing out that the heat flux is not divergence-free due to Joule heating.

2.2. Boundary conditions

In our system, the temperature, electric potential, normal electric current, and normal energy flux are all continuous across the interface, thus

$$T_1=T_2, \tag{7}$$

$$\phi_1=\phi_2, \tag{8}$$

$$J_{\perp1}=J_{\perp2}, \tag{9}$$

$$J_{E\perp1}=J_{E\perp2}, \tag{10}$$

in which the symbol $\perp$ donates normal to the interface, and the subscripts 1 and 2 represent the quantities within lower and upper materials, respectively.

2.3. General solutions of two-dimensional thermoelectric problem

Substituting Eq. (2) into Eq. (5) leads to

$$\nabla^2\left(\phi+ST\right)=0. \tag{11}$$

Then, $\phi+ST$ can be expressed as

$$\phi+ST=\mathrm{Re}[f[z]], \tag{12}$$

where $\mathrm{Re}[f[z]]$ is the real part of $f[z]$, and $z=x+\mathrm{i}y$. Substituting Eq. (12) into Eq. (2), we have

$$J_x=-\frac{1}{2}\sigma\frac{\partial(f[z]+\overline{f[z]})}{\partial x}=-\frac{\sigma}{2}(f'[z]+\overline{f'[z]}), \tag{13}$$

$$J_y=-\frac{1}{2}\sigma\frac{\partial(f[z]+\overline{f[z]})}{\partial y}=-\frac{\sigma\mathrm{i}}{2}(f'[z]-\overline{f'[z]}), \tag{14}$$

in which $\overline{f[z]}$ and $f'[z]$ denote the conjugate and derivative of $f[z]$, respectively. Combining Eqs. (13) and (14), we have

$$J_x-\mathrm{i}J_y=-\sigma f'[z]. \tag{15}$$

Substituting Eq. (3) into Eq. (6), and noticing Eq. (5), we can simplify the relationship between the temperature and electric current density as

$$\nabla^2T=-\frac{J^2}{\sigma\kappa}. \tag{16}$$

Noticing Eq. (15), ∇^2T can be expressed by $f[z]$ as

$$\nabla^2T=-\frac{\sigma}{\kappa}f'[z]\overline{f'[z]}. \tag{17}$$

Solving Eq. (17), we obtain

$$T=-\frac{\sigma}{4\kappa}f[z]\overline{f[z]}+g[z]+\overline{g[z]}+N, \tag{18}$$

where $g[z]$ is an arbitrary complex function, and N is an arbitrary real constant which donates the uniform temperature field. The electric potential can be derived by substituting Eq. (18) into Eq. (12) as

$$\phi=\frac{\sigma S}{4\kappa}f[z]\overline{f[z]}+\frac{1}{2}\left(f[z]+\overline{f[z]}\right)-S\left(g[z]+\overline{g[z]}\right)-SN. \tag{19}$$

Finally, the thermal flux and energy flux can be deduced from Eqs. (3), (4), (15), (18), and (19) as

$$J_{Qx}-\mathrm{i}J_{Qy}=\sigma f'[z]\left[\frac{\overline{f[z]}}{2}\left(\frac{\sigma S}{2\kappa}f[z]+1\right)-S\left(2\,\mathrm{Re}[g[z]]+N\right)\right]-2\kappa g'[z], \tag{20}$$

$$J_{Ex}-\mathrm{i}J_{Ey}=-\frac{\sigma}{2}f[z]f'[z]-2\kappa g'[z]. \tag{21}$$

Up to this point, the temperature/electric potential fields as well as the electric/thermal/energy flux have been expressed by two unknown functions $f[z]$ and $g[z]$. As such, if the two analytic complex functions $f[z]$ and $g[z]$ can be derived, the fields of temperature, electric potential, heat flow, energy flux, and electric current can then be determined, and the problem is completely solved.

3. Solutions for a bi-layered thermoelectric medium

To be specific, we consider a bi-layered thermoelectric medium, as shown in Fig. 1. The thermoelectric properties of layers 1 and 2 are σ_1, S_1, κ_1 and σ_2, S_2, κ_2, respectively. Our goal is to determine the refraction law of the electric current. To this end, at the far field in phase 1, the medium is subjected to imposed electric current J_x^∞ , J_y^∞ , and energy flux J_{Ex}^∞ , J_{Ey}^∞. Furthermore, the two analytic functions introduced earlier, $f[z]$ and $g[z]$, are denoted as $f_1[z]$, $g_1[z]$ in phase 1 and $f_2[z]$, $g_2[z]$ in phase 2 to be distinguished from each other.

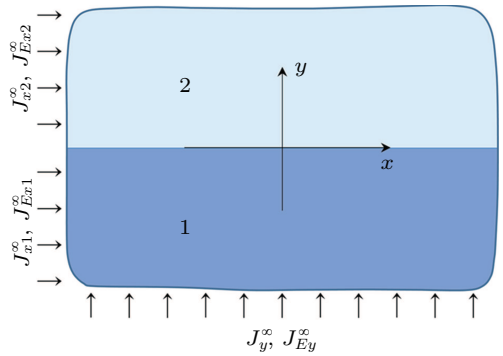


Fig. 1. (color online) Schematic diagram of a bi-material thermoelectric medium.

By noticing the far field loadings, analytic functions $f_i[z]$ and $g_i[z]$ can be expressed as

$$f_1[z] = A_0 + A_1 z, \tag{22}$$
$$f_2[z] = B_0 + B_1 z, \tag{23}$$
$$g_1[z] = C_1 z + C_2 z^2, \tag{24}$$
$$g_2[z] = D_1 z + D_2 z^2, \tag{25}$$

where A_0 and B_0 are arbitrary real constants. According to the far field loadings and Eqs. (15) and (21), the unknown coefficients A_1 and C_1 can be determined as $A_1 = -(J_x^\infty - \mathrm{i}J_y^\infty)/\sigma_1$ and $C_1 = -(J_{Ex}^\infty - \mathrm{i}J_{Ey}^\infty)/(2\kappa_1) - \sigma_1 A_0 A_1/(4\kappa_1)$. Due to this, the temperature fields and electric potential fields in media 1 and 2 can be rewritten as

$$T_1 = -\frac{\sigma_1}{4\kappa_1}|A_0 + A_1 z|^2 + 2\,\mathrm{Re}\left[C_1 z + C_2 z^2\right] + N, \tag{26}$$
$$T_2 = -\frac{\sigma_2}{4\kappa_2}|B_0 + B_1 z|^2 + 2\,\mathrm{Re}\left[D_1 z + D_2 z^2\right] + N_*, \tag{27}$$
$$\phi_1 = \frac{\sigma_1 S_1}{4\kappa_1}|A_0 + A_1 z|^2 + \mathrm{Re}\left[A_0 + A_1 z\right] - 2S_1\,\mathrm{Re}\left[C_1 z + C_2 z^2\right] - S_1 N, \tag{28}$$
$$\phi_2 = \frac{\sigma_2 S_2}{4\kappa_2}|B_0 + B_1 z|^2 + \mathrm{Re}\left[B_0 + B_1 z\right] - 2S_2\,\mathrm{Re}\left[D_1 z + D_2 z^2\right] - S_2 N_*, \tag{29}$$

where N_* is a real constant which represents a uniform temperature field in the upper material.

In addition, the electric current density, energy flux, and thermal flux can be rewritten as

$$J_{x1} - \mathrm{i}J_{y1} = -\sigma_1 A_1, \tag{30}$$
$$J_{x2} - \mathrm{i}J_{y2} = -\sigma_2 B_1, \tag{31}$$

$$J_{Qx1} - \mathrm{i}J_{Qy1} = \frac{\sigma_1 A_1 \left(A_0 + \overline{A_1 z}\right)}{2}\left[\frac{\sigma_1 S_1}{2\kappa_1}\left(A_0 + A_1 z\right) + 1\right] - 2\kappa_1\left(C_1 + 2C_2 z\right) - \sigma_1 S_1 A_1\left(2\,\mathrm{Re}\left[C_1 z + C_2 z^2\right] + N\right), \tag{32}$$

$$J_{Qx2} - \mathrm{i}J_{Qy2} = \frac{\sigma_2 B_1 \left(B_0 + \overline{B_1 z}\right)}{2}\left[\frac{\sigma_2 S_2}{2\kappa_2}\left(B_0 + B_1 z\right) + 1\right] - 2\kappa_2\left(D_1 + 2D_2 z\right) - \sigma_2 S_2 B_1\left(2\,\mathrm{Re}\left[D_1 z + D_2 z^2\right] + N_*\right), \tag{33}$$

$$J_{Ex1} - \mathrm{i}J_{Ey1} = -\frac{\sigma_1}{2}A_1\left(A_0 + A_1 z\right) - 2\kappa_1\left(C_1 + 2C_2 z\right), \tag{34}$$

$$J_{Ex2} - \mathrm{i}J_{Ey2} = -\frac{\sigma_2}{2}B_1\left(B_0 + B_1 z\right) - 2\kappa_2\left(D_1 + 2D_2 z\right). \tag{35}$$

Substituting Eqs. (26)–(35) into interfacial conditions Eqs. (7)–(10), and comparing the coefficients of the same power of z^k, we obtain the following coefficients:

$$B_0 = \left(\frac{\sigma_1 A_0^2}{4\kappa_1} - N\right)(S_1 - S_2) + A_0,$$
$$N_* = \frac{A_0 - B_0}{S_1 - S_2} + \frac{\sigma_2 B_0^2}{4\kappa_2},$$
$$B_1 = -\left(\frac{J_x^\infty}{\sigma_1} - \frac{\mathrm{i}J_y^\infty}{\sigma_2}\right) - \frac{(S_1 - S_2)\left(A_0 J_x^\infty - J_{Ex}^\infty\right)}{\kappa_1},$$
$$C_2 = \frac{J_x^{\infty 2} + J_y^{\infty 2} + 2\mathrm{i}J_x^\infty J_y^\infty}{8\sigma_1\kappa_1},$$
$$D_1 = -\frac{\left(A_0 J_x^\infty - J_{Ex}^\infty\right)\left[B_0\sigma_2\left(S_1 - S_2\right) - 2\kappa_2\right]}{4\kappa_1\kappa_2} - \frac{B_0\sigma_2 J_x^\infty + \mathrm{i}\sigma_1\left(B_0 J_y^\infty - 2J_{Ey}^\infty\right)}{4\sigma_1\kappa_2},$$
$$D_2 = \frac{1}{8\sigma_2\kappa_2}\left[\frac{\sigma_2\left(S_1 - S_2\right)\left(A_0 J_x^\infty - J_{Ex}^\infty\right)}{\kappa_1} + \frac{\sigma_2 J_x^\infty + \mathrm{i}\sigma_1 J_y^\infty}{\sigma_1}\right]^2 + \frac{J_y^{\infty 2}}{4\sigma_2\kappa_2}.$$

This set of equations solves the problems completely, leading to the full determination of the field distributions inside materials 1 and 2.

4. The refraction law of electric current, heat flux, and energy flux

We now consider the field distributions within media 1 and 2, specifically the current density, energy flux, heat flux, temperature, and potential given by Eqs. (26)–(35). The spatial variations of these field variables can be better appreciated

by an algebraic expansion of these equations using the nonzero coefficients derived in Section 3. In particular, the electric current density of media 1 and 2 are determined from Eqs. (30) and (31) as

$$J_{x1} - \mathrm{i}J_{y1} = J_x^{\infty} - \mathrm{i}J_y^{\infty}, \tag{36}$$

$$J_{x2} - \mathrm{i}J_{y2} = \sigma_2 \left[\left(\frac{J_x^{\infty}}{\sigma_1} - \frac{\mathrm{i}J_y^{\infty}}{\sigma_2} \right) + \frac{(S_1 - S_2)\left(A_0 J_x^{\infty} - J_{Ex}^{\infty}\right)}{\kappa_1} \right]. \tag{37}$$

It can be seen that the current is uniform within media 1 and 2, while the density and direction of the current in these two media are different. The incident angle in material 1 is defined as

$$\tan\theta_1 = \frac{J_{x1}}{J_{y1}} = \frac{J_x^{\infty}}{J_y^{\infty}}. \tag{38}$$

Then the refracted angle in material 2 can be expressed as

$$\tan\theta_2 = \frac{J_{x2}}{J_{y2}} = \sigma_2 \left[\frac{\tan\theta_1}{\sigma_1} + \frac{(S_1 - S_2)}{\kappa_1} \left(A_0 \tan\theta_1 - \frac{J_{Ex}^{\infty}}{J_y^{\infty}} \right) \right]. \tag{39}$$

Thus, the refraction law of electric current is

$$\frac{\tan\theta_2}{\tan\theta_1} = \frac{\sigma_2}{\sigma_1} + \frac{\sigma_2 (S_1 - S_2)}{\kappa_1} \left(A_0 - \frac{J_{Ex}^{\infty}}{J_x^{\infty}} \right), \tag{40}$$

which indicates that the refraction angle of the current depends not only on σ_2/σ_1, but also on $J_{Ex}^{\infty}/J_x^{\infty}$.

The refractive index, on the other hand, can be expressed by θ_1 and θ_2 as

$$\left| \frac{J_2}{J_1} \right| = \frac{\cos\theta_1}{\cos\theta_2}. \tag{41}$$

Equation (41) clearly shows that the current densities within media 1 and 2 are different from each other, and their ratio varies with the incident angle θ_1, since θ_2 also varies with θ_1, as expressed in Eq. (39). Using the refraction of the current, we can control the current density in each medium. For example, we maintain the incident current density equal to the optimal current density of medium 1, and then adjust the current density in medium 2 by adjusting the incidence angle. Finally, the current density in each medium can approach the optimal current density in this medium.

An important calculation result is shown in Fig. 2, with the material parameters detailed in Table 1, which clearly reveals that the refractive index $|J_2/J_1|$ varies with the incidence angle θ_1 in a wide range, thus providing enough space to adjust the current density in medium 2.

Table 1. Material parameters of thermoelectric samples.[29,30]

Sample	$\sigma/\mathrm{S\cdot m^{-1}}$	$S/\mu\mathrm{V\cdot K^{-1}}$	$\kappa/\mathrm{W\cdot m^{-1}\cdot K^{-1}}$
BiSbTe	27700	213	0.7
Bi_2Te_3	110000	200	1.6

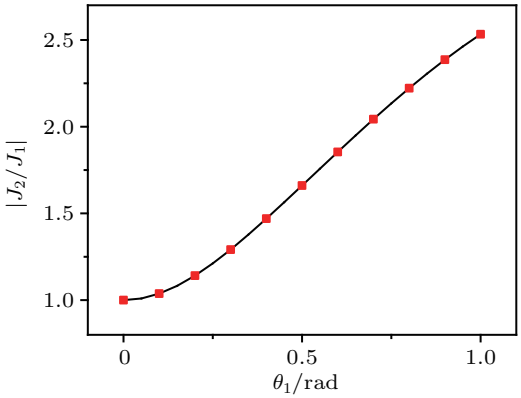


Fig. 2. (color online) $|J_2/J_1|$ varies with θ_1.

From Eqs. (33) and (35), the refracted angle of heat flux θ_2' and energy flux θ_2'' can be expressed as

$$\tan\theta_2' = \frac{\dfrac{\sigma_2 S_2 (A_0 - B_0) - \kappa_2}{\kappa_1} \left(A_0 \tan\theta_1 - \dfrac{J_{Ex}^{\infty}}{J_y^{\infty}} \right) + \dfrac{\sigma_2 S_2 (A_0 - B_0) \tan\theta_1}{\sigma_1 (S_1 - S_2)}}{\dfrac{A_0 S_2 - B_0 S_1}{S_1 - S_2} + \dfrac{J_{Ey}^{\infty}}{J_y^{\infty}}}, \tag{42}$$

$$\tan\theta_2'' = \frac{J_y^{\infty}}{J_{Ey}^{\infty}} \left[\frac{B_0 \sigma_2 (S_1 - S_2) - \kappa_2}{\kappa_1} \left(A_0 \tan\theta_1 - \frac{J_{Ex}^{\infty}}{J_y^{\infty}} \right) + \frac{B_0 \sigma_2}{\sigma_1} \tan\theta_1 \right]. \tag{43}$$

Although the expression of the heat flux refraction angle (Eq. (42)) is significantly different from that of the current refraction angle (Eq. (39)), the numerical results in Fig. 3 show that there is only a slight difference between them. The heat flux refraction also affects the energy conversion efficiency. The inconsistency between the heat flux and current direction usually leads to the decrease of efficiency, but this effect is weak. Generally speaking, the current refraction plays a major role in improving the efficiency.

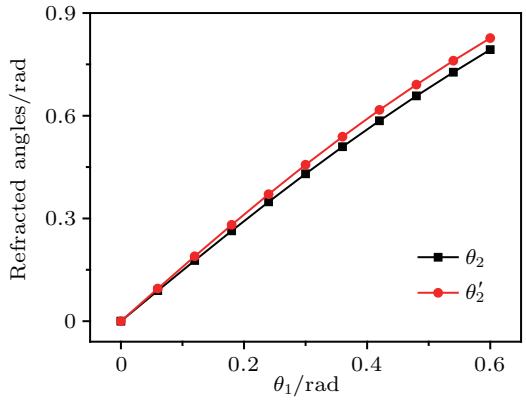


Fig. 3. (color online) Refracted angles of electric current θ_2 and heat flux θ_2' versus incident angle θ_1.

5. Conversion efficiency improved by current refraction

The conversion efficiency is also calculated to demonstrate the analysis. In classical bi-layered thermoelectric systems, the electric current flows through the interface vertically and retains its direction, which leads to a uniform electric current density in the whole system. In our new system, as shown in Fig. 4(b), the electric current refraction occurs at the interface, both the density and the direction of the current change, and the shape of the system is also altered to adapt to the refraction of the current. In the classical bi-layered thermoelectric system, the conversion efficiency can be expressed as[17]

$$\eta = \frac{\int_c^d \phi_2 J_2 \mathrm{d}s - \int_a^b \phi_1 J_1 \mathrm{d}s}{\int_a^b J_{Q1} \mathrm{d}s}. \tag{44}$$

In the new system, the conversion efficiency is

$$\eta^* = \frac{\int_{c^*}^{d^*} \phi_2^* J_2^* \mathrm{d}s - \int_{a^*}^{b^*} \phi_1^* J_1^* \mathrm{d}s}{\int_{a^*}^{b^*} J_{Q1}^* \mathrm{d}s}. \tag{45}$$

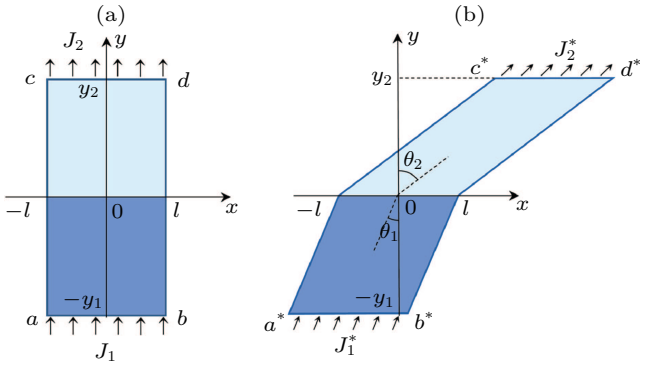


Fig. 4. (color online) (a) Classical bi-layered thermoelectric system. (b) New bi-layered thermoelectric system.

We can compare the conversion efficiency of the new bi-layered thermoelectric system with the maximum conversion efficiency of the classical bi-layered thermoelectric system in Fig. 5, with $y_1 = y_2 = 0.01$ m, $l = 0.0025$ m, $T_c = 300$ K, and $T_h = 500$ K, where θ_1 is the incidence angle, and $|J^\infty|$ equals to the optimal current density of medium 1. It is again evident that the current densities in different components can be adjusted independently, which is impossible for the classic bi-layered thermoelectric system. By adjusting the incidence current density and incidence angle, the upper bound of the conversion efficiency is significantly improved. Besides, as the incident angle increases, the conversion efficiency first rises to the maximum and then falls down, which indicates the existence of the optimal incidence angle.

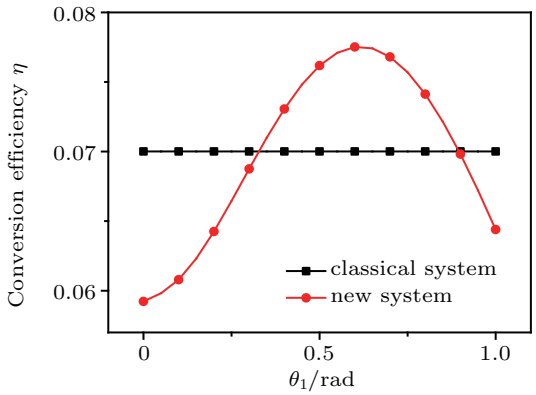


Fig. 5. (color online) Conversion efficiency versus θ_1 at $T_c = 300$ K and $T_h = 500$ K when J_1 is the optimal electric current in the lower material.

6. Conclusion

The problem of current refraction at the interface is studied in this paper. The relationships between the incidence angle, the refraction angle, and the refractive index are discussed in detail. We also propose a new model based on the conception of current refraction, wherein the current densities in two components can be adjusted independently, thus the optimal current density can be matched in both components, and the conversion efficiency can be significantly increased. In the new model, components with dissimilar compatibility factors can also be combined into efficient thermoelectric generators. These results point to a new route for high efficiency thermoelectric composites.

References

[1] Luan Y Q, Yang W, Xiao P, Ma Z F and Wang H P 2014 *Applied Mechanics and Materials* **716** 1457
[2] De Backer J, Bolmsjö G and Christiansson A K 2014 *The International Journal of Advanced Manufacturing Technology* **70** 375
[3] He W, Wang S, Li Y and Zhao Y 2016 *Energy Conversion and Management* **129** 240
[4] Kristiansen N R and and Nielsen H K 2010 *Journal of electronic materials* **39** 1746
[5] Liu L, Lu X S, Shi M L, Ma Y K and Shi J Y 2016 *Solar Energy* **132** 386
[6] Zheng X F, Yan Y Y and Simpson K A 2013 *Applied Thermal Engineering* **53** 305
[7] Bhandari C M and Rowe D M 1980 *Contemporary Physics* **21** 219
[8] Sharma S, Dwivedi V K and Pandit S N 2014 *International Journal of Green Energy* **11** 899
[9] Tiwari P, Gupta N and Gupta K M 2013 *Advanced Materials Research* **685** 161

[10] Harman T C and Honig J M 1967 *Thermoelectric and Thermomagnetic Effects and Applications* (New York: McGraw-Hill)
[11] Pei J, Zhang B P, Li J F and Liang D D 2017 *J. Alloys Compd.* **728** 694
[12] Zhang K, Zhang Q, Wang L, Jiang W and Chen L D 2017 *J. Alloys Compd.* **725** 563
[13] Zhang Y X, Ge Z H and Feng J 2017 *J. Alloys Compd.* **727** 1076
[14] Hochbaum A I, Chen R K, Delgado R D, Liang W J, Garnett E C, Najarian M, Majumdar A and Yang P D 2008 *Nature* **451** 163
[15] Chen J, Zhang G and Li B W 2010 *Nano Lett.* **10** 3978
[16] Chen J, Zhang G and Li B W 2012 *Nano Lett.* **12** 2826
[17] Mahan G D and Lyon Jr H B 1994 *J. Appl. Phys.* **76** 1899
[18] Yan H and Toshima N 1999 *Chemistry Letters* **28** 1217
[19] Antonik M, O'Connor B T and Ferguson S 2016 *Journal of Thermal Science and Engineering Applications* **8** 021022
[20] Rao A M, Ji X and Tritt T M 2006 *MRS Bulletin* **31** 218
[21] Snyder G J and Ursell T S 2003 *Physical review letters* **91** 148301
[22] Song K, Song H P and Gao C F 2018 *J. Appl. Phys.* **123** 124105
[23] Mahan G D 2013 *Phys. Rev. B* **87** 045415
[24] Yang Y, Xie S H, Ma F Y and Li J Y 2012 *J. Appl. Phys.* **111** 013510
[25] Yang Y, Ma F Y, Lei C H, Liu Y Y and Li J Y 2013 *Appl. Phys. Lett.* **102** 053905
[26] Song K, Song H P and Gao C F 2017 *Chin. Phys. B* **26** 127307
[27] Callen H B 1960 *Thermodynamics: An Introduction to the Physical Theories of Equilibrium Thermostatics and Irreversible Thermodynamics* (New York: Wiley)
[28] Milton G W 2002 *The Theory of Composites* (Cambridge: Cambridge University Press)
[29] Ahmad K, Wan C and Al-Eshaikh M A 2017 *J. Electron. Mater.* **46** 1348
[30] Antonova E E and Looman D C 2005 *ICT 2005. 24th International Conference on IEEE,* June 19–23, 2005, Clemson, USA, p. 215